Combustion Stability Analysis of Preburners During Engine Shutdown

Kair-Chuan Lim* and Paul E. George†
University of Tennessee, Knoxville, Tennessee 37916

Low-frequency combustion instability, known as chugging, is consistently experienced during shutdown in the fuel and oxidizer preburners of the Space Shuttle main engines (SSME). Such problems only occur during the helium purge of the residual oxidizer from the preburner manifolds during the shutdown sequence. Possible causes and triggering mechanisms are analyzed, and details in modeling the fuel preburner chug are presented in this report. A linearized, one-dimensional, lumped parameter chugging model capable of predicting the chug occurrence is discussed, and the predicted results are presented and compared to experimental work. In addition to predicting the actual instability, a parametric study of the various parameters such as chamber pressure, fuel and oxidizer temperatures, and the effective bulk modulus of the liquid oxidizer are considered in analyzing the fuel preburner chug. Particular attention has been given to such parameters as fuel and oxidizer temperatures since these vary with engine thrust at shutdown. The analyses show that chugging is likely to be affected by fuel and oxidizer conditions during SSME shutdown. The chug occurs when fuel, oxidizer and helium temperatures, and flow rates pass into an unstable region where the critical time delay is matched to the system resonances.

Nomenclature

$\dot{m}$ = mass flow rate
s = Laplace variable
I = imaginary root
K = pressure ratio
M = Mach number
P = pressure
R = real root
T = temperature
V = volume
Z = linearized output impedance
ρ = gas density
τ = combustion time delay
θ = gas residence time
γ = specific heat ratio
σ = vaporization time
Φ = equivalence ratio
ω = frequency

Subscripts

c = combustion chamber
e = exit
f = fuel
fb = fuel burned
fi = fuel injected
hg = hot gas manifold
o = oxidizer
ob = oxidizer burned
oi = oxidizer injected
t = total
p = constant pressure
Φ = constant equivalence ratio

Superscripts

$\sim$ = perturbation quantity
$-$ = mean value
$'$ = critical value

Presented as Paper 87-1776 at the AIAA/SAE/ASME/ASEE 23rd Joint Propulsion Conference, San Diego, CA, June 29-July 2, 1987; revision received Oct. 10, 1989; accepted for publication Feb. 19, 1990.

*Research Assistant, Department of Mechanical and Aerospace Engineering; currently Senior Propulsion Engineer, Martin Marietta Manned Space Systems, New Orleans, LA. Member AIAA.

†Assistant Professor, Department of Mechanical and Aerospace Engineering; currently Research Scientist, Battelle Columbus Division, Columbus, OH.

Introduction

THE current design of the Space Shuttle main engines (SSME) uses two preburners that are known to be stable for steady-state operation at the required full power level. These preburners, however, exhibit a low-frequency ($f < 200$ Hz) pressure pulsation, known as chugging, while the oxidizer manifold is being purged during the shutdown sequence. Because these pulsations are of low amplitude and occur at chamber pressure very much less than the design pressure, they are not considered to be life threatening. However, there is an interest in understanding the chug behavior to assist in analyzing advanced engine designs. This paper describes a model developed to study the primary independent parameters affecting chugging instabilities.

Cryogenic liquid hydrogen enters the engine from the external tank via a low-pressure pump, which supplies enough head to prevent cavitation of the three-stages high-pressure fuel pump. The high-pressure fuel pump discharges the hydrogen at approximately 7000 psia at full power level. The hydrogen is used to cool the nozzle, throat, and main combustion chamber before entering the preburner at a temperature of 1027 K. The majority of the fuel flows through the preburners and is partially burned before entering the main combustion chamber.

The oxidizer (LOX) follows a similar path but is not used for cooling purposes and enters the main combustion chamber directly. The pressure at the outlet of the single-stage oxidizer pump is approximately 4400 psia. The oxygen is fed directly into the main combustion chamber operating at 3277 psia. A portion of the oxidizer is supplied to the preburner pump, which supplies oxygen at 6850 psia to the fuel and oxidizer preburners.

The three main engines supply a combined nominal thrust of 4,780,000 lbf at rated power level. Engine power is controlled by throttling the oxidizer flow to the two preburners via the fuel and oxidizer preburner oxidizer valves (FPOV and OPOV). The power available to the turbopumps and hence reactant flow rate is controlled by the supply of oxygen to the preburners.

Under steady-state conditions, the preburners are operating at fuel-rich conditions with an approximate equivalence ratio of six. Combustion is extinguished in the preburner and in the main combustion chamber by closing the OPOV in the oxidizer line. The closing of the OPOV causes the suspension of the oxidizer flow to the combustion chamber, thus extinguishing combustion prior to fuel cutoff.

The engines are throttled back prior to shutdown in flight operations due to maximum acceleration limitations of the shuttle. The ground test firings on the SSME are frequently shutdown from 100% rated power level. For a nominal shutdown, the OPOV is closed first and followed shortly by the closure of the FPOV. The preburners are isolated from the oxidizer system once the two preburner oxidizer valves are closed. The only oxidizer available to the preburners is the residual trapped in the line and manifold volume between the valve and combustion chamber. This residual oxygen is cleared into the preburners by a helium purge.

The chug usually begins about 2.3–2.5 s after the cutoff command is given on ground test. The conditions for flight test data were not available; however, the situation should be similar to ground testing except that, in flight, engine cutoff usually occurs at lower power levels. Although the chug appears to correspond to the closing of the main oxidizer valve (MOV), it is important to note that the preburners are completely isolated from the oxidizer system by the time MOV closes.

The amplitude, frequency, and duration of the instability appear to be dependent on shutdown conditions, particularly the helium compressibility and fuel temperatures.[1] Since the chug occurs on shutdown, loss of performance on the SSME is of no major concern. The chug peak pressure never exceeds 1000 psia, whereas the combustion chambers are designed for pressures in excess of 6000 psia. Because of this fact, chugging has received very little attention. However, failure of the augmented spark ignitor line on the fuel preburner has been linked to the chug. Further, new engine designs can benefit from an effective stability analysis technique.

Method of Approach

The primary objective of this work was to improve on analysis techniques for rocket instability in the preburners of liquid propellant rockets. Particular emphasis was given to the fuel preburner of the SSME. Although chugging is observed in both preburners, the fuel preburner chug is more severe than the oxidizer preburner chug. Triggering mechanisms and the methods for chug elimination are also presented. System variables such as chamber pressure, fuel flow rate, oxidizer flow rate, and fuel and oxidizer temperatures were varied, and their effect on the fuel preburner chug is presented. Chemical kinetics in the combustion process were assumed to be infinitely fast and therefore were neglected in the analysis.

The analysis presented by Crocco and Cheng[2] and Harrje and Reardon[3] are more extensive in the analysis of combustion instabilities than earlier models. Their models concentrated on design criteria that should be avoided during engine construction. The early developments of combustion instability analysis were linearized models based upon the work done by Crocco and Cheng.[2] These models have shown that chugging is critically sensitive to combustion time delay and low injector pressure drops. The compressibility of the feed system was also considered as a principal contributor to the chug. The approach taken by Szuch[4] in analyzing main combustion chamber chugging instabilities appeared to be the most effective of the technique available. The computer program written by Szuch was used as a foundation for this research. The method was adapted to the SSME propellant flow arrangement including the unchocked exit flow in the SSME fuel preburner.

Following the analysis of Szuch,[4] the characteristic equation describing the stability of a bipropellant rocket system is derived from the nonlinear differential equation governing propellant flow then reduced to a quadratic equation. The quadratic formula, which is a closed-form solution, is used to solve the characteristic equation. A high accuracy solution is obtained as no iterative process is required. The solution of the characteristic equation, utilizing critical system values, will result in the generation of a critical stability boundary. It is therefore possible to predict if the operating point of the fuel preburner is in the stable or unstable region. Only the complex roots with positive real parts are sought. Complex roots with positive real parts indicate that the system is unstable as an unbound amplitude is predicted. The imaginary part obtained provides the frequency of interest at the critical operating point.

Numerical Model

Analysis

The burnt gases in the fuel preburner of the SSME can be considered as an ideal gas, and the flow is determined by the conservation laws of mass, momentum, and energy. In the range of low frequencies pertaining to chugging, propagation of the pressure waves is assumed to be instantaneous; thus, the following fundamental assumptions for chugging can be stated:

1) The gas pressure is uniform throughout the combustion chamber and oscillates about a mean or steady-state value.

2) The temperature of the gases is constant and uniform regardless of the pressure oscillations, but depends on stoichiometry.

3) The time lag (or delay) is uniform; that is, it has the same value for all the propellant elements; and

4) The combustion of the propellant is infinitely fast once the droplet has evaporated and mixed; chemical kinetics are therefore neglected.

These four assumptions greatly simplify the analytical treatment of the combustion process; the introduction of assumptions 1) and 2) replace the momentum and energy equations, which therefore need not be considered. The introduction of assumptions 3) and 4) allow the finite droplet evaporation time to collapse to a single characteristic time. With the combustion proceeding infinitely fast, a quasi-steady-state process is assumed.

These assumptions reduce the formulation for the dynamics of the combustion process in the fuel preburner to be essentially governed by the balance of mass; that is, the rate of burned gas produced must be equal to the sum of the rate of ejection of gas out of the fuel preburner through the high pressure fuel turbine and the rate of mass accumulated in the preburner.

The schematic of the fuel preburner in Fig. 1 is used to illustrate the combustion process during shutdown of the SSME. Following shutdown, the oxidizer line is closed by a ball valve, and the residual oxidizer is purged by the helium.

The fuel and helium flow rates are determined by conditions upstream and downstream of the injector elements. The oxidizer vaporizes, mixes, and reacts with a small fraction of the fuel to produce a hot gas consisting primarily of H_2 and H_2O. The time interval that exists between liquid propellant injec-

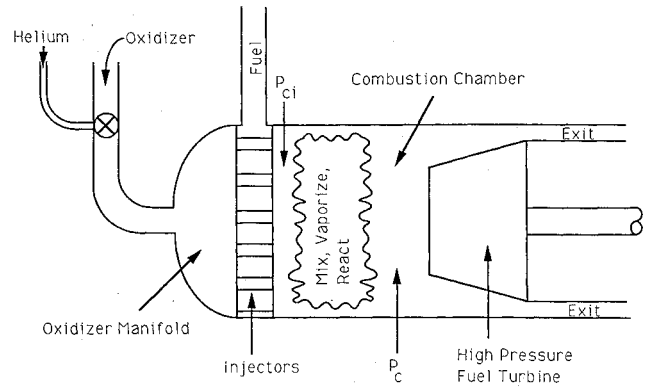

Fig. 1 Schematic of SSME fuel preburner combustion chamber.

tion and conversion to vaporized propellant is referred to as the vaporization time delay. The characteristic vaporization time delay σ_v, used in this model, is the time required for the conversion of 50% of the liquid propellant to the vaporized state. The gas phase mixing time delay σ_m is the time interval required for the conversion of vaporized propellant to burned gases. These time delays (σ_v and σ_m), which are functions of time, are assumed to be combined into a single characteristic time. The following equations are used to relate the rate of change of burned products to the injected propellant flow rates:

$$\dot{m}_{ob}(t) = \dot{m}_{oi}(t - \sigma_{vo} - \sigma_m) \tag{1}$$

$$\dot{m}_{fb}(t) = \dot{m}_{fi}(t - \sigma_{vf} - \sigma_m) \tag{2}$$

Using a one-dimensional lumped parameter approach, Harrje and Reardon[3] state that the basic governing equation is obtained from the conservation of mass. The conservation of mass written for the fuel preburner, assuming that all the reactants are burned, yields

$$\frac{\partial}{\partial t}[\rho V_c] = \dot{m}_{fb}(t) + \dot{m}_{ob}(t) - \dot{m}_e(t) \tag{3}$$

The helium purge is included in the $\dot{m}_{ob}$ term. Equation (3) is based on the assumption that the volume occupied by the liquid is very small compared to the total chamber volume and is valid only for low frequencies. The exit mass flow is given by[1]

$$\dot{m}_e(t) = C\sqrt{\frac{P_c}{T_c}\left[\left(\frac{P_{hg}}{P_c}\right)^{1.4286} - \left(\frac{P_{hg}}{P_c}\right)^{1.7143}\right]} \tag{4}$$

where C is an empirically determined coefficient, which is a function of turbine speed.

Since the gas density is a function of pressure and temperature, Eq. (3) is nonlinear and must be linearized to obtain the desired solution. Linearization of Eq. (3) is performed by assuming a small perturbation in the system variables about a steady-state operating point. Neglecting the products of perturbations yields the following equation:

$$\theta_g \frac{\partial}{\partial t}\left[\frac{\tilde{\rho}}{\bar{\rho}}\right] + \frac{\tilde{m}_e(t)}{\bar{m}_t(t)} = \frac{\tilde{m}_{fb}(t) + \tilde{m}_{ob}(t)}{\bar{m}_t(t)} \tag{5}$$

where the tilde superscripts are the perturbation quantities,

$$\theta_g = \frac{\bar{\rho} v_c}{\bar{m}_t} \tag{6}$$

is the gas residence time, and

$$\bar{m}_t(t) = \bar{m}_{fb}(t) + \bar{m}_{ob}(t) = \bar{m}_e(t) \tag{7}$$

is the total mean mass flow of the exhaust gases. Assuming that the gas behaves as an ideal gas, the first term on the left-hand side of Eq. (5) can be shown to be

$$\theta_g \frac{\partial}{\partial t}\left[\frac{\tilde{\rho}}{\bar{\rho}}\right] = \theta_g \frac{\partial}{\partial t}\left[\frac{\tilde{P}_c}{\bar{P}_c}\right] - \theta_g \frac{\partial}{\partial t}\left[\frac{\tilde{T}_c}{\bar{T}_c}\right] \tag{8}$$

Since the temperature perturbation is spatially variant, that is, the temperature at the combustion front and the exit of the preburner is different, the mean temperature perturbation should be integrated over the entire preburner combustion chamber. However, with assumption 2), stated earlier, the chamber temperature remains relatively constant on the time scale associated with chugging. Thus, the second term on the right-hand side of Eq. (8) goes to zero.

Utilizing the ideal gas law in Eq. (4), the second term on the left-hand side of Eq. (5) may be expressed as

$$\frac{\tilde{m}_e(t)}{\bar{m}_e(t)} = C1\left[\frac{\tilde{P}_c}{\bar{P}_c}\right] - \frac{1}{2}\left[\frac{\tilde{T}_c}{\bar{T}_c}\right] \tag{9}$$

where $C1$ is determined from input parameters and is a function of the specific heat ratio of the combustion products and pressure ratio found in Eq. (4).

Equations (5), (8), and (9) are combined to yield the following equation:

$$\theta_g \frac{\partial}{\partial t}\left[\frac{\tilde{P}_c}{\bar{P}_c}\right] + C1\left[\frac{\tilde{P}_c}{\bar{P}_c}\right] = \frac{\tilde{m}_{fb}(t) + \tilde{m}_{ob}(t)}{\bar{m}_t(t)} + \frac{1}{2}\left[\frac{\tilde{T}_c}{T_c}\right] \tag{10}$$

The last term of Eq. (10) becomes

$$\frac{\tilde{T}_c}{\bar{T}_c} = \frac{\tilde{\Phi}}{T_c}\left[\frac{\partial \bar{T}_c}{\partial \Phi}\right]_p \frac{\tilde{\Phi}}{\bar{\Phi}} + \frac{\tilde{P}_c}{\bar{T}_c}\left[\frac{\partial \bar{T}_c}{\partial \bar{P}_c}\right]_\Phi \frac{\tilde{P}_c}{\bar{P}_c} \tag{11}$$

and with the temperature being a weak function of the chamber pressure, Eq. (11) reduces to

$$\frac{\tilde{T}_c}{\bar{T}_c} = \frac{\tilde{\Phi}}{\bar{T}_c}\left[\frac{\partial \bar{T}_c}{\partial \Phi}\right]_p \frac{\tilde{\Phi}}{\bar{\Phi}} \tag{12}$$

The equivalence ratio perturbation may be expressed in terms of the oxidizer and fuel mass flux perturbations as

$$\frac{\tilde{\Phi}}{\bar{\Phi}} = \frac{(1+\bar{\Phi})\tilde{m}_{ob}}{\bar{\Phi}\bar{m}_t} - \frac{(1+\bar{\Phi})\tilde{m}_{fb}}{\bar{m}_t} \tag{13}$$

Equations (1), (2), (10), (11), and (13) are combined to yield the following equation, which relates the chamber pressure to the injected propellant flow rate:

$$\theta_g \frac{\partial}{\partial t}\left[\frac{\tilde{P}_c}{\bar{P}_c} + C1\left[\frac{\tilde{P}_c}{\bar{P}_c}\right] = X\tilde{m}_{fi}(t - \tau_o)\right.$$

$$\left. + Y\dot{m}_{oi}(t - \tau_f)\right. \tag{14}$$

where $\tau = (\sigma_v + \sigma_m)$ is the combustion time delay, and

$$X = \frac{1}{\bar{m}_t}\left[1 + \frac{1}{2}\frac{(1+\bar{\Phi})}{\bar{T}_c}\left(\frac{\partial \bar{T}_c}{\partial \Phi}\right)\right] \tag{15}$$

$$Y = \frac{1}{\bar{m}_t}\left[1 - \frac{1}{2}\frac{\bar{\Phi}(1+\bar{\Phi})}{\bar{T}_c}\left(\frac{\partial \bar{T}_c}{\partial \bar{\Phi}}\right)\right] \tag{16}$$

The Laplace transformation of Eq. (14) is

$$[\theta_g s + C1]\tilde{P}_c(s) = \bar{P}_c X\tilde{m}_{oi}(s)e^{-\tau_o s} + \bar{P}_c Y\tilde{m}_{fi}(s)e^{-\tau_f s} \tag{17}$$

The perturbation in the injected propellant flow rate is related to the perturbation in the chamber pressure at the injector face by

$$\tilde{m}_{oi}(s) = -\frac{\tilde{P}_{ci}(s)}{z_o(s)} \tag{18}$$

$$\tilde{m}_{fi}(s) = -\frac{\tilde{P}_{ci}(s)}{Z_f(s)} \tag{19}$$

where subscripts i represent the injector face.

The total and static chamber pressure at the injector face are related by their definition as

$$P_{ct} = p_{cs}\left[1 + \frac{(\gamma-1)}{2}M^2\right]^{\frac{\gamma}{(\gamma-1)}} \tag{20}$$

where subscripts t and s represent the total and static pressures, respectively.

The static pressure in the combustion chamber and at the injector face are written in terms of the Mach number as

$$\frac{p_{ci}}{p_c} = \frac{1 + \gamma M_c^2}{1 + \gamma M_{ci}^2} \tag{21}$$

Assuming that M_{ci} is small (i.e., a large chamber), Eqs. (20) and (21) can be combined to yield the following pressure ratio (K):

$$\frac{P_{ci}}{P_c} = \frac{1 + \gamma M_c^2}{\left[1 + \dfrac{(\gamma - 1)}{2} M_c^2\right]^{\dfrac{\gamma}{(\gamma - 1)}}} = K \tag{22}$$

Assuming that there is no loss in the total chamber pressure, Eqs. (17), (18), (19), and (22) are combined to yield the following result:

$$\tilde{P}_c = \frac{\bar{P}_c}{\theta_g s + C1 + \dfrac{\bar{P}_c XK}{Z_o(s)} e^{-\tau_o s} + \dfrac{\bar{P}_c YK}{Z_f(s)} e^{-\tau_f s}} \tag{23}$$

The preceding equation relates the steady-state average chamber pressure to the perturbed chamber pressure in the system. The existence of the chug is inferred by an unbounded pressure perturbation; that is, $\tilde{P}_c(s)$ approaches infinity. This condition is obtained by setting the denominator of Eq. (23) to zero, resulting in

$$-1 = \left(\frac{\bar{P}_c XK}{Z_o(s)} e^{-\tau_o s} + \frac{\bar{P}_c YK}{Z_f(s)} e^{-\tau_f s}\right) \div \theta_g s + C1 \tag{24}$$

Equation (24) is the characteristic equation describing the stability of any bipropellant rocket system with unchocked exit flow and is applicable to the SSME fuel preburner system when the proper choice of K, P_c, X, Y, Z, and $C1$ is made.

The characteristic equation is solved only for complex roots having positive real parts (exponential growth). Appearance of these roots indicates that chugging is present and defines the stability boundary. The appearance of a negative root signifies that the system is stable. The imaginary root defines the frequency at which the chug occurs. A minimum frequency of 75 Hz was selected, and the stability program solved the characteristic equation for positive real complex roots. If no non-negative roots are found, the procedure is repeated with another selected frequency. The positive real part of the complex root is related to the respective pressure drops (P_{fi}/P_c and P_{oi}/P_c). The region to the right of the boundary, outside the envelope, corresponds to stable operation, whereas the region within the envelope is unstable. The shape of the stability boundary is such that an increase in oxidizer or fuel pressure drop stabilizes the preburner. This model only predicts the probability of instabilities, but provides no information on the limits of the chug amplitude.

Solution of Characteristic Equation

The solution of the characteristic equation is performed by separating the output impedances $Z_o(s)$ and $Z_f(s)$ into their real and imaginary parts. Letting $s = j\omega$, the characteristic equation is separated, which results in the following real and imaginary equations [Eqs. (25) and (26), respectively]:

$$-C1 = \frac{P_c XKR_o \cos(\omega\tau_o) - P_c XKI_o \sin(\omega\tau_o)}{R_o^2 + I_o^2} + \frac{P_c YKR_f \cos(\omega\tau_f) - P_c YKI_f \sin(\omega\tau_f)}{R_f^2 + I_f^2} \tag{25}$$

$$\omega\theta_g = \frac{P_c XKI_o \cos(\omega\tau_o) + P_c XKR_o \sin(\omega\tau_o)}{R_o^2 + I_o^2} + \frac{P_c YKI_f \cos(\omega\tau_f) + P_c YKR_f \sin(\omega\tau_f)}{R_f^2 + I_f^2} \tag{26}$$

where

$$Z_o(j\omega) = R_o + jI_o \tag{27}$$

$$Z_f(j\omega) = R_f + jI_f \tag{28}$$

For the frequency range of interest, Eqs. (25) and (26) are solved for two critical parameters R_o and R_f. The real parts of R_o and R_f are selected because they can be related to the injector flow resistances $2\Delta P/m_o$, which are independent of the frequency.

It can be shown that the characteristic equation reduces to the following quadratic equation relating the critical value of the real part of the oxidizer impedance R_o' to the imaginary feed system impedances I_o' and I_f' for a specified frequency:

$$\begin{aligned} &R_o'^2\left[F - \frac{I_f}{P_c YK}\left(C1^2 + (\omega'\theta_g)^2\right)\right] \\ &+ R_o'\left\{\frac{2XI_f}{Y}\left[C1\cos(\omega'\tau_o) + \omega'\theta_g \sin(\omega'\tau_o)\right] - P_c XK \sin(\omega'\tau_o - \omega'\tau_f)\right\} \\ &+ \left\{I_o^2 F - I_o P_c XK \cos(\omega'\tau_o - \omega'\tau_f) - \frac{I_o^2 I_f}{P_c YK}\left(C1^2 + \omega'^2\theta_g^2\right) - \frac{I_f P_c X^2 K}{Y} - \frac{2XI_o I_f}{Y}\right. \\ &\left.\times\left[C1\sin(\omega'\tau_o) - \omega'\theta_g\cos(\omega'\tau_o)\right]\right\} = 0 \end{aligned} \tag{29}$$

where

$$F = \omega'\theta_g \cos(\omega'\tau_f) - C1 \sin(\omega'\tau_f) \tag{30}$$

The solution of Eq. (29) is used to compute the critical real part of the fuel impedance R_f via

$$R_f' = \frac{R_o' P_c YK \cos(\omega'\tau_f) + I_o P_c YK \sin(\omega'\tau_f) + I_f P_c XK \sin(\omega'\tau_o) - \omega'\theta_g R_o' I_f + C1 I_o I_f}{\omega'\theta_g I_o + C1 R_o' - P_c XK \cos(\omega'\tau_o)} \tag{31}$$

The solution of Eqs. (29) and (31) can be related physically to the injector element and feed system being studied. The imaginary variables I_o and I_f must be computed, at each specified critical frequency, prior to the solution of Eqs. (29) and (31). Equations (25–30) have been translated into a Fortran computer program, CHUGTEST. The program solves the characteristic equation utilizing the closed-form quadratic formula. A range of possible chugging frequencies must be specified to initiate the program. The frequency range for chugging

instabilities is between 75 to 200 Hz; thus frequencies higher than 200 Hz are neglected.

Results and Discussion

The analysis of the SSME fuel preburner chug during shutdown is in agreement with experimental results. The frequency for the fuel preburner chug (Fig. 2) varies from 115 to 145 Hz as determined by counting the peaks over a selected time segment. The mean frequency of the chug over the entire time interval is 125 Hz. The chug frequency predicted by the model differed by 10% from the mean value obtained experimentally. This disagreement was due to the conservative linearized approach taken in the analysis. The predicted frequencies are in good agreement at the two end regions of the chug since a low amplitude chug is approximately linear.

The onset of the chugs due to chamber pressure variations were analyzed. The chamber pressure was varied from 3.45×10^6 Pa (500 psia) to 5.86×10^6 Pa (850 psia) as input parameters into the program. The stability boundary computation was performed with a starting frequency of 75 Hz and is incremented by 0.1 Hz to calculate the required pressure drops. A stability boundary curve was generated by computing the fuel injector pressure drop and the oxidizer injector pressure drop at the critical frequency of interest; thus the stability of the nominal operating point can be determined.

The parametric studies were performed utilizing two different bulk moduli. The bulk moduli used in the model were gaseous helium and LOX. Since helium is an inert gas, the compressibility of helium may provide the necessary condition for the chug.

When low oxidizer and fuel temperatures [$T_o = 40$ K, $T_f = 40$ K (72°R)] were utilized as inputs, with varying chamber pressure, the system was inevitably unstable even at low pressures with a frequency of 115 and 121 Hz, shown in Figs. 3 and 4, respectively. The ratio of fuel injector pressure drop to chamber pressure (P_{fi}/P_c) of the operating point was never below the minimum point of the stability boundary.

The effect of fuel and oxidizer temperatures on the stability of the system was also considered. At a chamber pressure of 4.48×10^6 Pa (650 psia), which is the mean chugging pressure, the oxidizer temperature was subjected to a variation ranging from 40 to 120 K, whereas the fuel temperature was kept relatively low at 40 K. The variation of oxidizer temperature with low fuel temperature did not stabilize the fuel preburner system; however, it was noted that operations at high fuel and oxidizer temperatures (120 and 100 K, respectively) stabilized the system. High oxidizer and fuel temperatures cause partial

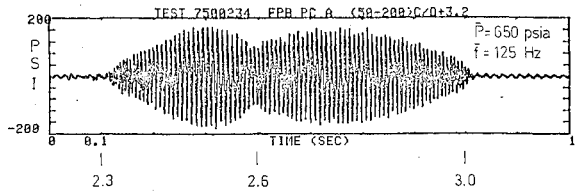

Fig. 2 Fuel preburner pressure trace during chugging.

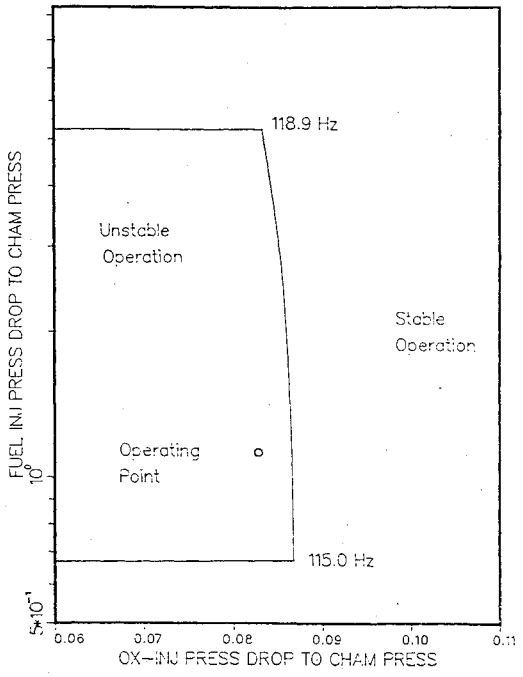

Fig. 3 Unstable operation with low fuel and oxidizer temperatures at mean chugging pressure.

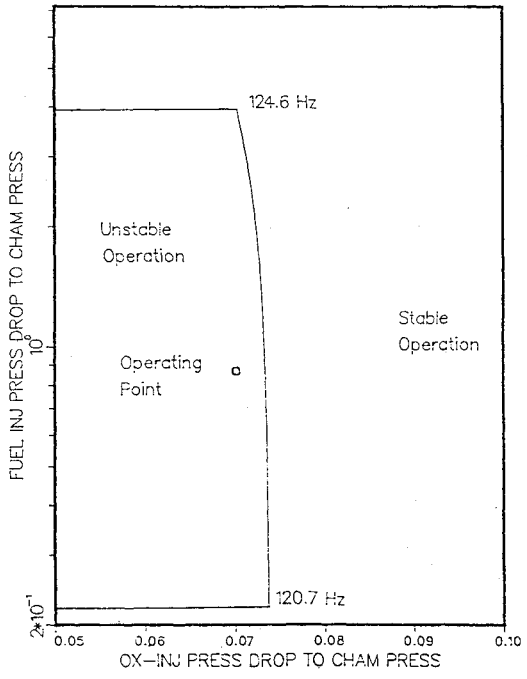

Fig. 4 Unstable operation with low fuel and oxidizer temperatures at mean chugging pressures.

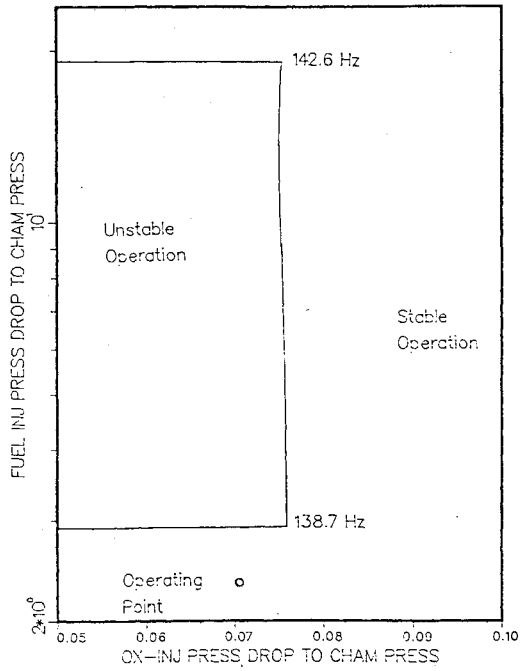

Fig. 5 Stable operation with increased fuel and oxidizer temperatures at mean chugging pressure.

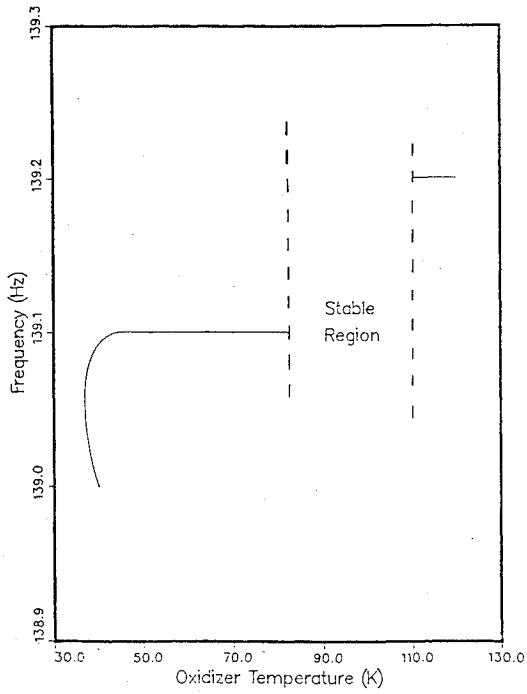

Fig. 6 Variation of chugging frequency with oxidizer temperature.

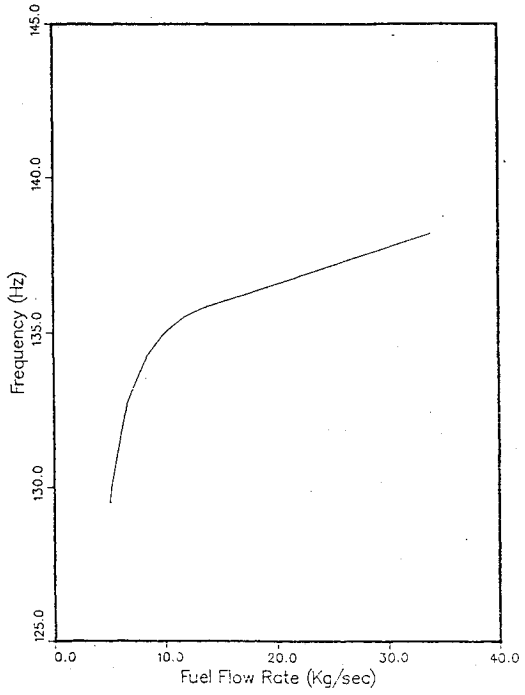

Fig. 7 Variation of chugging frequency with fuel flow rate.

vaporization of the liquid oxidizer and hence smaller droplet radius. Vaporization and mixing times are thus decreased with the smaller droplet radius. The stability of the system, probably due to the proper mixing of reactants, could be achieved by increasing propellant temperatures even at the mean pressure where chugging is prevalent.

Since it is undesirable to work with high oxidizer temperatures, several test cases were run to determine if oxidizer temperatures could be reached and yet maintain stability. It was noted that stability was achieved with higher fuel temperatures while other parameters remained constant. This result presented in Fig. 5 shows the fuel temperature at 150 K, while oxidizer temperature was lowered to 86 K.

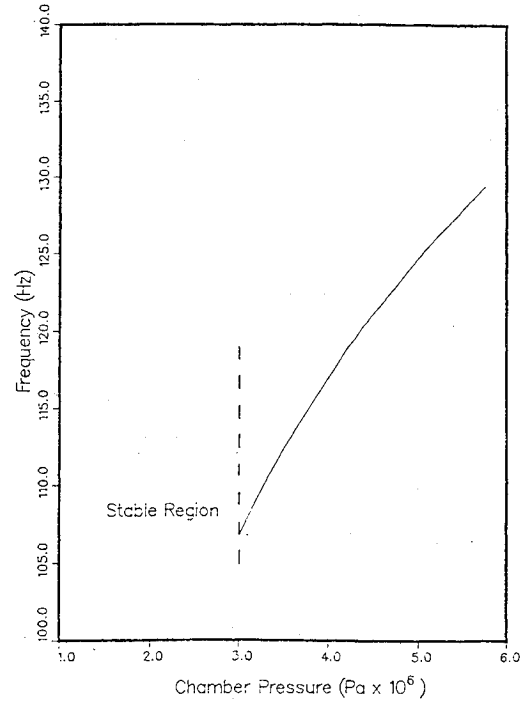

Fig. 8 Variation of chugging frequency with chamber pressure.

At the nominal operating point, reduction of fuel flow rate is unlikely to inhibit the chug since chugging exists at relatively high fuel flow rate (equivalence ratio = 6). The mean droplet radius, being an inverse function of fuel flow rate, increases with fuel flow reduction causing an increase in vaporization and mixing time. Reducing fuel flow changed the frequency of the chugging but did not shift the operating point nearer to the stable region.

The influence of varying the oxidizer flow rate on the chug was studied. Although there is no oxidizer feed during shutdown, as the FPOV is already closed, the helium flow rate is considered as the oxidizer flow since it clears the residual oxidizer from the lines and manifold. This is possible because the residual oxidizer flow rate is equivalent to that of helium using the appropriate density value. The model predicted that stability was achieved at low pressures with increased flow rates.

The model was also tested with the bulk modulus of liquid oxygen at conditions where chugging exists. There were no stability boundaries generated for those conditions signifying stable operation. The frequency range of 75 to 200 Hz was tested with variations in the chamber pressure, oxidizer, and fuel temperatures. The instability which was prevalent at previous operating conditions, with the bulk modulus of helium, was eliminated utilizing the bulk modulus of liquid oxygen. This shows that the chug depends not only on operating conditions but also on the helium purge conditions, specifically the compressibility of the helium.

Figures 6, 7, and 8 show the variation of chugging frequency with oxidizer temperature, fuel flow rate, and chamber pressure, respectively. Figure 6 shows that stable operation was achieved with oxidizer temperatures between 80 to 115 K. Temperatures below 80 K resulted in unstable operation at a frequency of 139 Hz. Figure 7 shows that the system could not be stabilized by variation of fuel flow rate. The two endpoints of the curve were arbitrarily selected for this parametric study. Figure 8 shows that stable operation is permissible at low pressures. The chugging frequency increases monotonically with increased chamber pressure up to 5.76×10^6 (830 psia).

The preceding parametric studies show that chugging is likely to be affected by conditions at shutdown through the fuel and oxidizer temperatures. On the basis of this analysis, it appears that the fuel preburner chugging observed during shutdown is initiated when the fuel, oxidizer, and helium temperature and flow rates pass into an unstable region, i.e., a region where the critical time delay associated with oxidizer evaporation/combustion is matched to the system resonances. Chugging may be terminated by decaying pressures. Although the analysis in this model was simplified, it provides a basic understanding of the occurrence of the SSME fuel preburner chug and the parameters to be investigated further for chug elimination. The analysis can be easily extended to encompass other stability questions, including advanced designs for propulsive gas turbines.

Acknowledgment

The support of NASA Marshall Space Flight Center is gratefully acknowledged. This work was performed at the University of Tennessee, Knoxville.

References

[1]George, P. E., II, "An Investigation of Space Shuttle Main Engine Shutdown Chugging Instability," NASA/ASEE Summer Faculty Fellowship Program, Research Rpts. 1984, NASA CR-171317, Jan. 1985.

[2]Crocco, L., and Cheng, S., "Theory of Combustion Instability in Liquid Propellant Rocket Motors," Butterworths Scientific Publications, London, 1956.

[3]Harrje, D. T., and Reardon, F. H., "Liquid Propellant Rocket Combustion Instability," NASA SP-194, 1972.

[4]Szuch, J. R., "Digital Computer Program for Analysis of Chugging Instabilities," NASA TN-D-7026, Dec. 1970.